

Long-term continuous energy injection in the afterglow of GRB 060729 *

Ming Xu¹, Yong-Feng Huang¹ and Tan Lu²

¹ Department of Astronomy, Nanjing University, Nanjing 210093, China; hyf@nju.edu.cn

² Purple Mountain Observatory, Chinese Academy of Sciences, Nanjing 210008, China

Received 2009 June 15; accepted 2009 September 28

Abstract A long plateau phase and an amazing level of brightness have been observed in the X-ray afterglow of GRB 060729. This peculiar light curve is likely due to long-term energy injection in external shock. Here, we present a detailed numerical study of the energy injection process of magnetic dipole radiation from a strongly magnetized millisecond pulsar and model the multi-band afterglow observations. It is found that this model can successfully explain the long plateaus in the observed X-ray and optical afterglow light curves. The sharp break following the plateaus could be due to the rapid decline of the emission power of the central pulsar. At an even later time ($\sim 5 \times 10^6$ s), an obvious jet break appears, which implies a relatively large half opening angle of $\theta \sim 0.3$ for the GRB ejecta. Due to the energy injection, the Lorentz factor of the outflow is still larger than two even at 10^7 s after the GRB trigger, making the X-ray afterglow of this burst detectable by Chandra even 642 d after the burst.

Key words: gamma rays: bursts — ISM: jets and outflows

1 INTRODUCTION

GRB 970228 is the first gamma-ray burst (GRB) with a detected X-ray afterglow (Costa et al. 1997). Optical (van Paradijs et al. 1997) and radio afterglows (Frail et al. 1997) have also been unprecedentedly detected from this event. The relativistic internal and external shock model is the most successful model to explain these violent events (Rees & Mészáros 1994; Piran 1999; Zhang 2007). It is also widely believed that long GRBs could be due to the collapse of massive stars (Woosley 1993; Paczyński 1998; MacFadyen & Woosley 1999), and short GRBs could be connected with the coalescence of two compact objects (Eichler et al. 1989; Narayan et al. 1992; Gehrels et al. 2005; Nakar 2007).

The X-ray telescope (XRT) onboard Swift reveals that the X-ray afterglows of GRBs generally show a canonical behavior, with five components in the observed X-ray afterglow light curves, i.e., steep decay phase, shallow decay phase, normal decay phase, post jet break phase and X-ray flares (Zhang et al. 2006; Nousek et al. 2006). The conventional models for the shallow decay phase are energy injection from strongly magnetized millisecond pulsars (Dai & Lu 1998; Zhang & Mészáros 2001; Liang et al. 2007; Lyons et al. 2009) or from ejecta with a highly dispersed Lorentz factor distribution (Rees & Mészáros 1998; Sari & Mészáros 2000).

At 19 : 12 : 29 UT on 2006 July 29, GRB 060729 triggered the *Swift* Burst Alert Telescope (BAT) and was quickly located (Grupe et al. 2006). This event had a duration of $T_{90} = 116 \pm 10$ s (Parsons et al. 2006) and a redshift of $z = 0.54$ (Thoene et al. 2006). The isotropic energy release in the rest-frame in

* Supported by the National Natural Science Foundation of China.

the 1 keV–10 MeV band was $E_{\text{iso}} = 1.6 \times 10^{52}$ erg for a standard cosmology model with $\Omega_M = 0.27$, $\Omega_\Lambda = 0.73$ and a Hubble constant of $H_0 = 71 \text{ km s}^{-1} \text{ Mpc}^{-1}$.

One of the distinguishing properties of GRB 060729 is that it has a long flat phase in the X-ray afterglow light curve (Grupe et al. 2007). Another prominent characteristic of GRB 060729 is its brightness. It could be observed by *Chandra* even 642 d after the burst trigger (Grupe et al. 2009). Grupe et al. (2009) compared the X-ray afterglow of GRB 060729 with other bright X-ray afterglows and concluded that GRB 060729 was an exceptionally long-lasting event. Actually, the brightness of the X-ray afterglow of GRB 060729 was not extraordinary at early times ($t < 30\,000$ s), but it became the brightest of all GRBs 30 000 s after the trigger.

In view of the long plateau phase (500 s–30 000 s) and the late time ($> 30\,000$ s) brightness of GRB 060729, a strong and long-term continuous energy injection is implied (Liang et al. 2007; Grupe et al. 2007, 2009). Grupe et al. (2007) presented an extensive study of this peculiar event and made a detailed analysis of the pulsar-type energy injection for this plateau. However, at that time there were only 125 d of data and the jet break still had not appeared. In this paper, we use the energy injection model that involves dipole radiation from a strongly magnetized millisecond pulsar to explain the special behavior of the multi-band afterglow of GRB 060729. The new data observed by *Chandra* (Grupe et al. 2009) will be incorporated. We calculate the X-ray and optical (*U*-band, *B*-band and *V*-band) afterglow light curves in detail, and compare them with the observations. In Section 2, we briefly describe the energy injection model. In Section 3, we present our detailed numerical results. Finally, Section 4 gives our conclusions and a discussion.

2 ENERGY INJECTION FROM A STRONGLY MAGNETIZED MILLISECOND PULSAR

Due to the strong magnetic field and rapid rotation, a new-born millisecond pulsar will radiate a huge amount of energy through magnetic dipole emission. This energy can be comparable to or even larger than the initial energy of the main GRB. Detailed discussions of this process have been given by Dai & Lu (1998) and Zhang & Mészáros (2001).

Through magnetic dipole radiation, the new-born pulsar in the center of the GRB fireball will lose its rotational energy. The radiation power evolves with time as

$$L = L_0 \left(1 + \frac{t}{T}\right)^{-2}, \quad (1)$$

where L_0 is the initial luminosity, i.e., the radiation power at the time $t = 0$. T is the characteristic spin-down timescale.

The initial luminosity depends on the parameters of the pulsar as

$$L_0 = 4.0 \times 10^{47} \text{ erg s}^{-1} (B_{\perp,14}^2 P_{-3}^{-4} R_6^6), \quad (2)$$

where $B_{\perp,14} = B_s \sin \vartheta / 10^{14}$ G, B_s is the strength of the dipole magnetic field at the surface of the pulsar, ϑ is the angle between the rotation axis and the magnetic axis, P_{-3} is the pulsar period in units of 10^{-3} s, and R_6 is the radius of the pulsar in units of 10^6 cm.

The characteristic spin-down timescale of the pulsar can be calculated from

$$T = 5.0 \times 10^4 \text{ s} (B_{\perp,14}^{-2} P_{-3}^2 R_6^{-6} I_{45}), \quad (3)$$

where I_{45} is the moment of inertia of the pulsar in units of 10^{45} g cm².

The total energy of the magnetic dipole radiation can be derived by integrating the emission power from $t = 0$ to $t \rightarrow \infty$

$$E_{\text{total}} = \int_0^\infty L dt = \int_0^\infty \left[L_0 \left(1 + \frac{t}{T}\right)^{-2} \right] dt = L_0 T. \quad (4)$$

3 NUMERICAL CALCULATION AND RESULTS

A convenient method to describe the dynamics and radiation processes of GRB afterglows has been proposed by Huang et al. (2000). It is appropriate for both radiative and adiabatic blastwaves, and in both ultra-relativistic and non-relativistic phases (Huang et al. 1999). Here, we modify their method accordingly so that it can be applicable to the energy injection scenario.

3.1 Dynamics

The overall dynamical evolution of GRB afterglows has been described by Huang et al. (1999, 2000). When the energy injection from a strongly magnetized millisecond pulsar is included, the deceleration of the external shock is mainly characterized by the following equation

$$\frac{d\gamma}{dm} = \frac{-(\gamma^2 - 1) + d(Lt)/d(mc^2)}{M_{ej} + \epsilon m + 2(1 - \epsilon)\gamma m}, \quad (5)$$

where γ is the bulk Lorentz factor of the shocked medium, m is the swept-up mass, M_{ej} is the initial ejecta mass, and ϵ is the radiation efficiency.

For simplicity, here we only consider the synchrotron emission from shock-accelerated electrons. To get the observed afterglow flux, we need to integrate the emission power over the equal arrival time surface determined by

$$\int \frac{1 - \beta \cos \Theta}{\beta c} dR \equiv t, \quad (6)$$

within the jet boundaries, where $\beta = \sqrt{\gamma^2 - 1}/\gamma$ and Θ is the angle between the velocity of the emitting material and the line of sight.

3.2 Numerical Results

Inserting Equation (1) into Equation (5), we can conveniently calculate the evolution of the external shock subject to the energy injection from a strongly magnetized millisecond pulsar. In this section, we assume that the circum-burst medium is homogeneous. We calculate the overall dynamical evolution of a uniform jet to deduce the X-ray and optical afterglow light curves, and try to give the best fit to the observations of GRB 060729.

To get the best fit, we find that we need to set the parameters of the central pulsar as follows. The radius is $R_6 = 1$. The rotation period is $P_{-3} = 1.49$. The magnetic field is $B_{\perp,14} = 2.72$. The moment of inertia is taken as $I_{45} \sim 2$, which is still typical for neutron stars (Datta 1988; Weber & Glendenning 1993). Then, according to Equations (2) and (3), the initial emission power and the spin-down timescale of the central pulsar are $L_0 = 6.0 \times 10^{47} \text{ erg s}^{-1}$, and $T = 30\,000 \text{ s}$ respectively. So, the energy injection power is $L = 6.0 \times 10^{47} \text{ erg s}^{-1} (1 + \frac{t}{30\,000 \text{ s}})^{-2}$.

In our calculations, we use the following parameters for the external shock of GRB 060729: the initial energy per solid angle $E_0 = 1.6 \times 10^{52}/4\pi \text{ erg}$, the initial Lorentz factor $\gamma_0 = 200$, the ISM number density $n = 0.2 \text{ cm}^{-3}$, the power-law index of the energy distribution of electrons $p = 2.48$, the luminosity distance $D_L = 3.12 \text{ Gpc}$, the electron energy fraction $\epsilon_e = 0.15$, the magnetic energy fraction $\epsilon_B = 0.0002$, the half opening angle of the jet $\theta = 0.3$, and the observing angle $\theta_{\text{obs}} = 0$. Here, the observing angle is defined as the angle between the line of sight and the jet axis.

Using the above parameter set, we can give a satisfactory fit to the multi-band afterglows of GRB 060729. In Figure 1, we first show the evolution of the Lorentz factor under energy injection from a strongly magnetized millisecond pulsar. We see that due to the continuous energy injection, the Lorentz factor of the outflow is still larger than 2 after 10^7 s . This means that the afterglow could be very bright even at very late stages.

Figure 2 illustrates the observed X-ray (0.3–10 keV) afterglow light curve of GRB 060729 and our best fit. We can see that the observed X-ray afterglow light curve is fitted very well. In particular, the

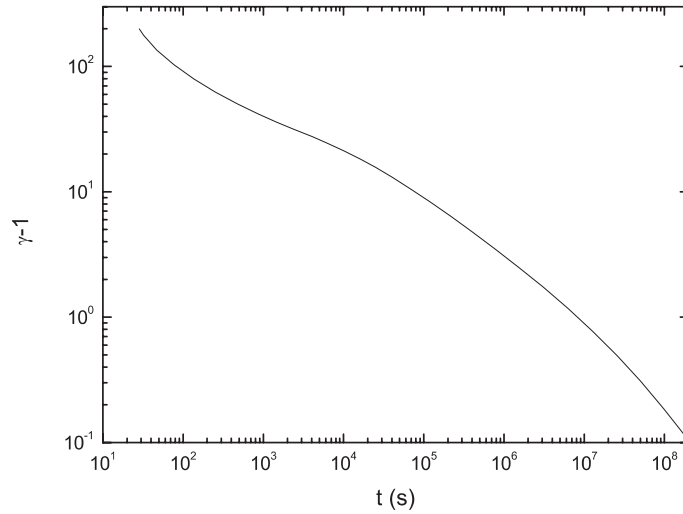


Fig. 1 Evolution of the bulk Lorentz factor of a jet with long-term energy injection from a strongly magnetized millisecond pulsar. The parameters used in this calculation are given in Sect. 3.2.

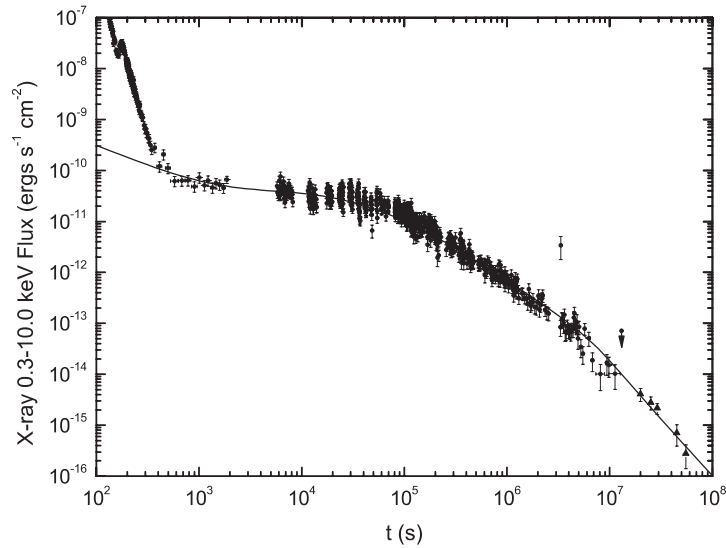


Fig. 2 Observed X-ray afterglow light curve of GRB 060729 and our best fit by using the energy injection model. The square points are observed data from *Swift* and the triangular points are observed data from *Chandra* (Grupe et al. 2009). The tail emission in the very early phase ($t < 400$ s) is not considered in our fit.

observed long plateau (~ 500 s – $30\,000$ s) is explained satisfactorily. This long flat phase results from long-term continuous energy injection from the magnetic dipole radiation of the strongly magnetized millisecond pulsar. After $30\,000$ s, the flat phase comes to an end and a break is seen in the light curve. The reason is that the pulsar has consumed most of its rotational energy on the spin-down timescale ($T = 30\,000$ s in our model), so that the power of energy injection decreases sharply at that time. An

obvious jet break is present at $t_j \sim 5 \times 10^6$ s. To produce such a late jet break, we find that the half opening angle of the jet should be $\theta = 0.3$, which is relatively large among known GRBs.

Figure 3 illustrates our fit to the observed optical afterglows of GRB 060729 by using the same parameters as in Figures 1 and 2. All the data points are taken from Grupe et al. (2007). We see that the observed optical afterglow can also be satisfactorily explained.

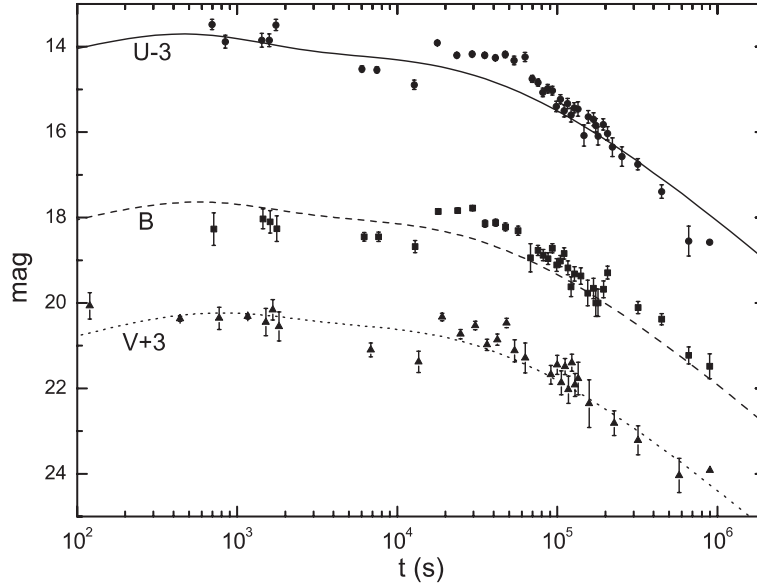


Fig. 3 Observed multi-band optical afterglow light curves of GRB 060729 and our best fit by using the energy injection model. Observed data points are taken from Grupe et al. (2007). The solid, dashed and dotted lines are our fit to the observed light curves in the three bands, respectively. Note that the U - and V -band light curves have been shifted by 3 magnitudes for clarity.

4 CONCLUSIONS AND DISCUSSION

We have shown that the observed special behavior of the afterglow of GRB 060729 can be explained well by using the energy injection model. Our study indicates that the central engine should be a strongly magnetized millisecond pulsar, which continuously supplies energy to the GRB ejecta via magnetic dipole radiation on a timescale of about 30 000 s. The observed multi-band afterglow light curves can be reproduced satisfactorily by this model. According to our calculations, the duration of the plateau phase in the afterglow light curve should correspond to the spin-down timescale of the pulsar ($T = 30\,000$ s). To further explain the observed jet break at $t_j \sim 5 \times 10^6$ s, we need a relatively large jet opening angle of $\theta = 0.3$.

From Equation (4), we can derive the total injected energy as $E_{\text{total}} = L_0 T = 1.8 \times 10^{52}$ erg. This energy is comparable to the initial isotropic energy release in the main burst phase ($E_{\text{iso}} = 1.6 \times 10^{52}$ erg). The long-term continuous energy injection makes GRB 060729 the brightest burst in the X-ray band at late stages. In fact, the X-ray afterglow can be observed even 642 d after the trigger (Grupe et al. 2009).

In optical bands, the afterglow light curves show some similar properties to the X-ray band. For example, a flat stage is present in the optical light curves. Generally, our model can give a satisfactory explanation for the optical afterglow. The time span of optical observations is very limited. We do not

have optical data for $t > 10^6$ s, so the jet break is still not observed in the optical band. However, note that extensive analyses with both the X-ray and optical data in recent years show that some of the jet-like breaks in the afterglow light curves are chromatic (Panaitescu et al. 2006; Liang et al. 2008). The nature of these breaks is then highly debatable. Thus, long-term monitoring of the multi-band afterglows is definitely necessary. Also note that the early UV-optical afterglow light curves of GRB 060729 show significant variations. This feature, however, is not seen in the X-ray light curve. This indicates that other regions may also contribute to the optical emission in this event.

In our current study, we have assumed that the energy injection is isotropic. Magnetic dipole radiation should actually be anisotropic. However, this kind of anisotropy is not significant and would not seriously affect the final results.

According to our numerical results, the Lorentz factor of the jet is still larger than 2 after 10^7 s. This is due to the continuous and long-term energy injection. As a result, the time that the afterglow of GRB 060729 enters the Newtonian phase is significantly delayed.

Energy injection models have been used to explain the afterglows of some GRBs, such as GRB 010222 (Björnsson et al. 2002), GRB 021004 (Björnsson et al. 2004), GRB 030329 (Huang et al. 2006) and GRB 051221A (Fan & Xu 2006), etc. The explanation of the afterglow from the short GRB 051221A also needs some kind of energy injection from a magnetar (Fan & Xu 2006). However, we note that the physical origin of the shallow decay segment is still hotly debated (Zhang 2007). Generally speaking, while the achromatic breaks in both the X-ray and the optical bands can be explained with conventional energy injection models, the chromatic breaks of this segment observed in many events strongly challenge these models (Liang et al. 2007). Alternative models that go beyond the conventional ones have been proposed (see Zhang 2007 for a review). It is interesting that a small fraction of XRT light curves are shown as a single power-law without canonical features (Liang et al. 2009). It has also been argued that the apparent difference between the canonical and single power-law XRT light curves may be due to the improper zero time effect on the canonical XRT light curves (Yamazaki 2009; Liang et al. 2009).

Acknowledgements We thank the anonymous referee for helpful suggestions. This work was supported by the National Natural Science Foundation of China (Grant Nos. 10625313 and 10473023) and the National Basic Research Program of China (973 Program, Grant No. 2009CB824800).

References

- Björnsson, G., Gudmundsson, E. H., & Jóhannesson, G. 2004, *ApJ*, 615, L77
 Björnsson, G., Hjorth, J., Pedersen, K., & Fynbo, J. U. 2002, *ApJ*, 579, L59
 Costa, E., Frontera, F., Heise, J., Feroci, M., in't Zand, J., et al. 1997, *Nature*, 387, 783
 Dai, Z. G., & Lu, T. 1998, *A&A*, 333, L87
 Datta, B. 1988, *Fund. Cosmic Phys.*, 12, 151
 Eichler, D., Livio, M., Piran, T., & Schramm, D. N. 1989, *Nature*, 340, 126
 Fan, Y. Z., & Xu, D. 2006, *MNRAS*, 372, L19
 Frail, D., Kulkarni, S. R., Nicastro, L., Feroci, M., & Taylor, G. B. 1997, *Nature*, 389, 261
 Gehrels, N., et al. 2005, *Nature*, 437, 851
 Grupe, D., et al. 2006, *GCN* 5365
 Grupe, D., et al. 2007, *ApJ*, 662, 443
 Grupe, D., et al. 2009, *ApJ*, submitted (arXiv: 0903. 1258)
 Huang, Y. F., Cheng, K. S., & Gao, T. T. 2006, *ApJ*, 637, 873
 Huang, Y. F., Dai, Z. G., & Lu, T. 1999, *MNRAS*, 309, 513
 Huang, Y. F., Gou, L. J., Dai, Z. G., & Lu, T. 2000, *ApJ*, 543, 90
 Liang, E. W., Lv, H. J., Zhang, B. B., & Zhang, B. 2009, *ApJ*, Submitted (arXiv:0902.3504)
 Liang, E. W., Racusin, J. L., Zhang, B., Zhang, B. B., & Burrows, D. N. 2008, *ApJ*, 675, 528
 Liang, E. W., Zhang, B. B., & Zhang, B. 2007, *ApJ*, 670, 565
 Lyons, N., O'Brien, P. T., Zhang, B., Willingale, R., Troja, E., & Starling, R. L. C. 2009, *MNRAS*, accepted (arXiv:0908.3798)

- MacFadyen, A. I., & Woosley, S. E. 1999, *ApJ*, 524, 262
Nakar, E. 2007, *PhR*, 442, 166
Narayan, R., Paczyński, B., & Piran, T. 1992, *ApJ*, 395, L83
Nousek, J. A., et al. 2006, *ApJ*, 642, 389
Paczynski, B. 1998, *ApJ*, 494, L45
Panaitescu, A., et al. 2006, *MNRAS*, 369, 2059
Parsons, A., et al. 2006, *GCN* 5370
Piran, T. 1999, *Phys. Rep.*, 314, 575
Rees, M. J., & Mészáros, P. 1994, *ApJ*, 430, L93
Rees, M. J., & Mészáros, P. 1998, *ApJ*, 496, L1
Sari, R., & Mészáros, P. 2000, *ApJ*, 535, L33
Thoene, C. C., et al. 2006, *GCN* 5373
van Paradijs, J., Granot, P., Galama, T., Kouveliotou, C., Strom R., et al. 1997, *Nature*, 386, 686
Weber, F., & Glendenning, N. K. 1993, *ApJ*, 390, 541
Woosley, S. E. 1993, *ApJ*, 405, 273
Yamazaki, R. 2009, *ApJ*, 690, L118
Zhang, B. 2007, *ChJAA (Chin. J. Astron. Astrophys.)*, 7, 1
Zhang, B., Fan, Y. Z., Dyks, J., et al. 2006, *ApJ*, 642, 354
Zhang, B., & Mészáros, P. 2001, *ApJ*, 552, L35